5-4. SACLA Beamlines

1. Operation status

SACLA was operated in FY2021 as scheduled, in contrast to the previous fiscal year, in which the facility shut down temporally because of the COVID-19 pandemic. International users have experienced significant difficulties with the facility visit because of the strict restrictions on entering Japan throughout the year. Collaborators based in Japan conducted some experiments when principal team members from abroad could not participate in the experiments on-site. In addition, the first pilot experiment using a remote system was successfully performed in 2021B as reported below. As a result, most experiments were conducted as scheduled in this fiscal year except for some canceled experiments proposed by international users. The user beamtime in FY2021 was ~6000 hours and is almost the same level as that before the pandemic.

Table 1 shows the operation parameters of the beamlines (BL1-3) at SACLA. BL1 is a soft X-ray (SX) free-electron laser (FEL) beamline using a dedicated linac. The other two beamlines, BL2 and BL3, are the hard X-ray FEL (XFEL) beamlines sharing the main linac. Those XFEL beamlines can be operated simultaneously because a fast-switching magnet changes the electron beam route pulse-by-pulse. Note that the magnet delivers the electron beam to the storage ring of SPring-8 constantly from the beginning of this fiscal year.

Table 1. Major operation parameters of SACLA [1].

	BL1	BL2 & BL3
Electron beam energy	800 MeV max.	8.5 GeV max.
Repetition	60 Hz max.	60 Hz max.
Undulator period	18 mm	18 mm
Undulator K value	2.1 max.	2.7 max.
Photon energy	40–150 eV	4–20 keV
Pulse duration	~30 fs	<10 fs

The major topics in upgrades on beamlines and experimental stations in this fiscal year are summarized in the following subsections. Some achievements are outcomes of close collaborations with external experts under the strategic programs below:

- SACLA/SPring-8 Basic Development Program
- SACLA Industry–Academy Partnership Program
- SACLA Research Support Program for Graduate Students

2. SX-FEL beamline (BL1)

2-1. Fully automated tuning of general beamline components

A fully automated tuning software program for general beamline components had been under development at BL1 after the development completion of a similar software program for BL2 and BL3. The software facilitates the routine beamline tunings, which had been manually conducted every beamtime by two to three facility staff. Here, the automated tunings include the alignment of the optical axis after the mirrors and measurements of the photon and pulse energies using the flat-field spectrometer and the gas intensity monitor, respectively. The software will be released officially in the middle of 2022.

2-2. Soft X-ray FEL microscope

A full-field microscope for SX-FEL was developed under the SACLA/SPring-8 Basic Development

Program and the SACLA Research Support Program for Graduate Students. The system is based on twin Wolter mirrors used as a condenser and an objective. Bright-field and full-field images can be captured with a field of view of 50 μm diameter and a spatial resolution of 200 nm in a single-shot exposure.

3. XFEL beamlines (BL2 and BL3)

3-1. First pilot experiment with newly developed remote system

The facility had started the system development to increase remote experiment capabilities and reduce loads of on-site collaborators since FY2020. The remote system allows access to the beamline equipment from outside facilities. After several demonstrations confirming the feasibility of the system, international users successfully performed the first pilot remote experiment at a high-power laser platform in EH6 in 2021B. During the beamtime, only a few users were on-site to prepare samples and care for user-owned instruments. The other users participated in the experiment remotely from their home countries. The remote operations include but are not limited to aligning samples, taking high-power laser shots with XFELs, and analyzing data via the high-performance computing (HPC) system. This remote system will be available on other experimental platforms in FY2022.

3-2. Automated tuning of beamline components and focusing mirror systems

A fully automated tuning system was officially released for general beamline components at BL2 and BL3 in FY2021 after a trial period of over a year. The system facilitates routine beamline tunings, for example, the alignment of the optical axis downstream of the offset mirrors or the double-crystal monochromator. During the automated tuning process at BL3, the photon energy is tuned finely by adjusting the gap of undulators.

The facility had also developed a semi-automated tuning system based on wavefront sensing by single-grating interferometry [2]. It was originally developed for aligning the mirrors of the 100 nm focusing system (so-called "100-exa") [3] at EH5 of BL3. In FY2021, the tuning system constantly helped improve the efficiency of experiments using the 100-exa system. The tuning system also started to be utilized for other nanofocusing systems, allowing for experiments using extreme focusing devices with flexible sample environments.

3-3. Development of sub-10 nm focusing system

As part of the SACLA Basic Development Program, a sub-10 nm focusing system using advanced Kirkpatrick–Baez mirrors arranged in the Wolter-type III geometry was developed at EH4c of BL3 to produce an X-ray laser field with an unprecedented intensity of ~10^{22} W/cm^2. The focusing system was tested in FY2021 with complete vacuum chambers for the mirrors and samples/diagnostics. The achieved focal profile was evaluated through various methods, including single-grating interferometry [2] and ptychography. Those methods presented similar profiles with a size of 7 × 7 nm^2 at full width at half maximum (FWHM), where we expected a peak intensity above 1 × 10^{22} W/cm^2. We also confirmed the excellent stability of the focusing properties both shot-by-shot and over a long time (~12 hours). The sub-10 nm focusing system was used for some pilot experiments in FY2021 and will be officially available for user

experiments in FY2022.

3-4. Timing stabilization of the femtosecond optical laser system for pump-probe experiments

A feedback system based on a balanced optical-microwave phase detector (BOMPD) working at a C-band frequency (5.7 GHz) has been installed in the mode-locked oscillator of the femtosecond optical laser system (sync-laser) in LH1 for BL3. The system realizes the timing jitter of about 50 fs (Fig. 1(a)) [4]. The long-term timing changes are compensated recursively by controlling the optical path of the oscillator output with a delay stage. The amount of the delay stage adjustment is estimated from the timing signal between XFEL and the optical laser pulses directly measured by the timing monitor [5]. The total timing fluctuation has been successfully reduced to the jitter level (~ 50 fs) in several hours (Fig. 1(b)). Owing to the new timing stabilization system, pump-probe experiments are performed without postprocessing for timing jitter mitigation in several tens of femtosecond resolution.

3-5. New experimental capabilities at the platforms with high-power optical lasers

The facility has been developing various geometry configurations for the X-ray diffraction (XRD) measurements of laser-shocked matter in EH5 equipped with a high-power nanosecond laser. In FY2021, a transmission geometry was newly established in addition to the existing reflection geometry. Another configuration, a side-on geometry, is under development for utilization in the coming year. An automated operation system on the platform has been developed and allows users to acquire data without the manual operation of the set of typical detectors.

In the high-power short-pulse laser platform in EH6, an instrument was calibrated to diagnose the spatial profiles of Kα emission at the sample. A quasi-monochromatic X-ray imager using a spherically bent quartz crystal has been tentatively operated to capture the images of Cu Kα X-rays, which are produced by the laser or XFEL irradiation to the Cu foil. The imager has been characterized and is ready to monitor the spatial overlaps of the laser and XFEL on shots.

4. Research highlights

4-1. Element-selective and symmetry-sensitive experiment with polarization-resolved soft X-ray SHG

Uzundal et al. performed the first demonstration of a polarization-resolved soft X-ray second-harmonic

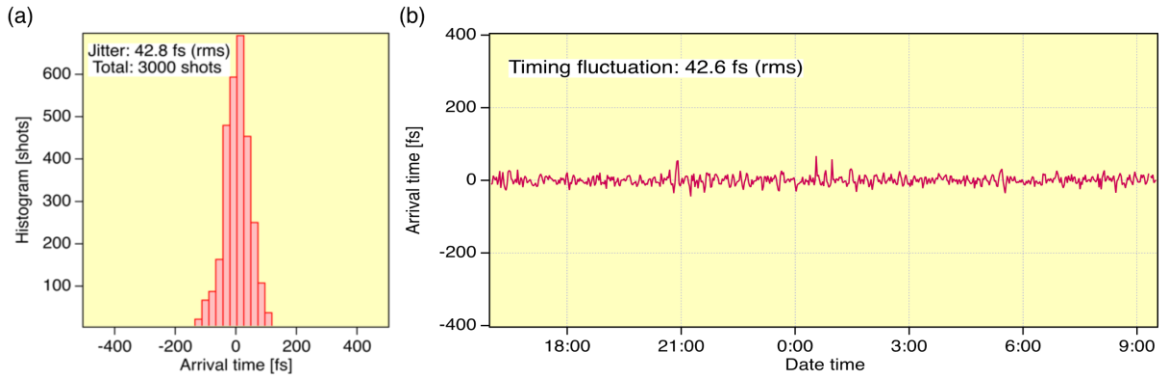

Fig. 1. (a) Histogram of the arrival time (3000 shots) [4]. (b) Trends of the arrival time while controlling the drift in 17 hours.

generation (SHG) experiment for the ferroelectric material $LiNbO_3$ at BL1 [6]. This experiment is an element-selective and symmetry-sensitive. The SHG measurements suggested that the displacement of Li ions, which leads to ferroelectricity, is accompanied by distortions to the NbO_6 octahedra that break the inversion symmetry of the Nb ion environment.

4-2. Characterization of a short-lived intermediate in N_2O generation by P450 NO reductase

Nitric oxide (NO) reductase catalyzes the reduction of NO to nitrous oxide (N_2O), which is known as an ozone-depleting substance and a greenhouse gas. Nomura et al. applied time-resolved IR spectroscopy and X-ray crystallography to P450 NO reductase in a short-lived intermediate state (*I*), where N–N bond formation and N–O bond cleavage are promoted [7]. On the basis of the coordination and electronic structures at the reaction site of the *I* state, they proposed a mechanism for N_2O generation with the aid of quantum mechanics/molecular mechanics calculations.

4-3. Pulse shortening of XFEL

Inoue et al. developed a nonlinear optical technique for shortening the duration of XFEL pulses [8]. Their technique employs atoms with core-hole vacancies (core-hole atoms) generated by inner-shell photoionization. The weak Coulomb screening in the core-hole atoms leads to saturable absorption, i.e., reduction in X-ray absorption at photon energies immediately above the absorption edge. By employing this phenomenon, they reduced the duration of XFEL pulses (photon energy: 9.000 keV, duration: 6–7 fs, and fluence: 2.0–3.5×10^5 Jcm^{-2}) by ~35%. Their results demonstrate that core-hole atoms are applicable to nonlinear X-ray optics, which is an important stepping stone for extending nonlinear optical technologies to the hard X-ray region.

4-4. Observation of ultrafast olivine-ringwoodite transformation within the shock-induced high-pressure state

Okuchi et al. investigated the ultrafast transformation mechanism yielding ringwoodite, the most typical high-pressure mineral in meteorites, with laser-driven compression and femtosecond X-ray diffraction [9]. They found that shock-compressed olivine transforms into ringwoodite through a nanosecond time scale. The transformation is a diffusionless process during shock release. Their results suggest that even nominally unshocked meteorites can contain recordings, as a form of ringwoodite, of high-pressure states from past collisions occurring throughout the evolution history of the solar system.

Inoue Ichiro[*1], Kubota Yuya[*1], Miyanishi Kohei[*1], Osaka Taito[*1], Owada Shigeki[*1,2], Togashi Tadashi[*1,2], Yabuuchi Toshinori[*1,2], Tono Kensuke[*1,2], and Yabashi Makina[*1,2]

[*1] XFEL Research and Development Division, RIKEN SPring-8 Center

[*2] XFEL Utilization Division, Japan Synchrotron Radiation Research Institute

References:

[1] Tono, K., et al. (2019). *J. Synchrotron Radiat.* **26**, 595.

[2] Yamada, J. et al. (2020). *Sensors* **20**, 7356.

[3] Yumoto, H. et al. (2020). *Appl. Sci.* **10**, 2611.

[4] Togashi, T. et al. (2020). *Appl. Sci*. **10**, 7934.

[5] Sato, T. et al. (2015). *Appl. Phys. Express* **8**, 012702; Katayama, T. et al. (2016). *Struct. Dyn.* **3**, 034301; Nakajima, K. et al. (2018). *J. Synchrotron Radiat.* **25**, 592; Katayama, T. et al. (2019). *J. Synchrotron Radiat.* **26**, 333.

[6] Uzundal, C. B. et al. (2021). *Phys. Rev. Lett.* **127**, 237402.

[7] Nomura, T. et al. (2021). *Proc. Natl. Acad. Sci. USA* **118**, e2101481118.

[8] Inoue, I. et al. (2021). *Phys. Rev. Lett.* **127**, 163903.

[9] Okuchi, T. et al. (2021). *Nat. Commun.* **12**, 4305.